Chapter VI

Biophysical relevance of nanoscale Gd_2O_3 systems

In the recent past, luminescent nanomaterials have accelerated scientific interest in the areas of labeling, sensing, and detecting single biomolecule as well as macromolecules. In particular, rare-earth oxide (REO) based nanostructures have immense potential in the field of biomedical engineering as they are capable of offering quality optical imaging and as contrast agents for magnetic resonance imaging (MRI) and thus have emerge as a vital asset in diagnostics and therapeutics [1,2]. Essentially, rare-earth materials have comparable luminescence features like semiconductor quantum dots (QDs) [3]. However, rare-earth oxides nanosystems enjoy a greater advantage over QDs due to exhibition of a narrow emission line width, a higher emission intensity response and a higher photostability response [4].

Gadolinium oxide (Gd_2O_3) is a well-known rare-earth sesquioxide [5]. While the system is thermally, chemically and mechanically stable and associated with low phonon energy (phonon cut off ~600 cm^{-1}), it can be used as a promising host for accommodating suitable dopants including RE ions [6]. It may be noted that, Gd possesses a maximum number of (seven) unpaired, 4*f* electrons ($^8S_{7/2}$) and give rise to a large electron magnetic moment [7] and no other element in the periodic table possess unpaired electrons similar to Gd [8]. Consequently, either in elemental or oxide form, it has emerged as the most preferred choice for use as MRI contrast agent [9].

A rapid growth in the application of advanced nanomaterials, particularly in the biomedical field has resulted numerous studies with respect to the toxicology aspect of nanosystems in biological environment [10]. Earlier, cytotoxicity aspect was evaluated using different oxide systems, such as, TiO_2 [11], ZrO_2, Al_2O_3 etc. [10] as well as metals, like Au, Ag nanoparticles [12,13]. Among different RE containing compounds, Gd_2O_3 and Dy_2O_3 nanosystems have also been successfully examined [14,15]. It is worth mentioning here that, nanoparticle-size, shape and morphology can have a strong influence as regards biocompatibility, cytotoxicity and cell viability. In this regard, one-dimensional (1D) elongated nanosystems, like nanorods, nanostrips, nanotubes etc. are expected to interact differently in cellular environment as compared to

the spherical nanoparticles. The relevance of fluorescent quantum dots has already been shown in bioimaging and diagnostics owing to cell-surface interactions [16-18]. In this chapter, we explore biophysical characteristics of Gd_2O_3 nanoparticles and nanorods with special emphasis on human lymphocytes. Furthermore, concentration dependent response of these nanosystems has been examined on known cancer cells with regard to control.

6.1 Biophysical characterization: Cytotoxicity and cell viability tests

The systematic biophysical work is as detailed below.

6.1.1 Isolation, culture, and treatment of lymphocytes

The cell viability effect of GNP and GNR was evaluated in human lymphocytes, isolated from the blood samples collected willingly. For this human blood with anti-coagulant was diluted with a phosphate buffer solution (PBS) (v/v 1:1). 3 mL histopaque (1.07 g-mL^{-1}) was taken in a centrifuge and were tipped on the histopaque layer. Subsequently, it was centrifuged at 400 g for 30 min and lymphocytes were collected from the buffy layer. The isolated lymphocytes were then washed thrice with 2 mL PBS followed by 2 mL RPMI-1640 media through centrifugation steps separately for 10 min at 250 g. The lymphocytes plates were then suspended in RPMI-1640, and viability was tested by the trypan blue exclusion method using a hemocytometer [19]. Cells were suspended in RPMI-1640 and 3×10^3 cells were seeded in 96 well plates with supplementation of 10% heat-inactivated FBS. Initially, cells were incubated (at ~37 °C in 5% CO_2) for 8 h in RPMI-1640 without FBS. The cells were then treated as per experimental requirement and maintained with the inclusion of FBS for 24 h.

6.1.2 Membrane stability assay

Human Blood was collected voluntarily; RBC was isolated from the blood samples and washed three times with PBS (pH =7.4) followed by centrifugation at 2000 rpm for 10 min. 2% Erythrocyte suspension (ES) was re-suspended in saline solution. The reaction mixture contained 100 µL of ES, 0.1% Triton X-100 and 25, 50 and 100 µg/ml of GNP and GNR was added to microfuge tubes,

after that incubated for 60 min at 37°C followed by cooling on ice under constant agitation. The release of hemoglobin was determined after centrifugation (~2000 rpm for 10 min) by photometric analysis of the supernatant at 576 nm. Complete hemolysis was achieved using 0.1% Triton X-100 yielding the 100% (positive control) and PBS yielding the 0% (negative control) hemolysis [20].

6.1.3 Cell culture and treatment condition

HepG2 (human liver hepatocellular carcinoma) cell line and breast cancer cell line MDA-MB231 were purchased from the National Centre for Cell Science (NCCS), Pune, India. HepG2 cells were cultured in DMEM medium (Himedia, India) containing 10% fetal bovine serum (Himedia, India,), 5% Penstrap Antibiotic solution (Himedia, India) were grown in an incubator in presence of 5% CO_2 and at a temperature of 37 ^oC, ensuring a stable environment. MDA-MB231 cells were cultured in L-15 Medium (Leibovitz) (Himedia, India) containing 10% fetal bovine serum, 100 U/ml penicillin, and 100 mg/L streptomycin. The cells were grown in an incubator kept at a temperature of ~ 37^{o}C. *In vitro* cytotoxicity of GNP and GNR was assessed using a standard MTT (3-(4,5-dimethyl-2-thiazolyl)-2,5- diphenyl-2-H-tetrazoliumbromide) assay with two cell lines (HepG2 and MDA-MB231 cells) counting 2 × 10^3 cells were seeded in a 96-well plate and treated with increasing concentrations (25, 50 and 100 µg/mL) of GNP and GNR, for 24 h (maintaining at ~37 °C, 5% CO_2). The cytotoxicity was determined by adding 10 µl of MTT [3-(4, 5-dimethylthiazol-2-yl)-2,5-diphenyl tetrazolium bromide] (0.5 mg/mL in PBS) to each well and incubated for 4 h. The medium was removed and 200 µl DMSO was added to each well and after 10 min of mechanical shaking, the optical density (OD) was measured at 570 nm using a plate reader. The viability was determined in relation to control cells cultured in drug-free media. All experiments were repeated at least three times and the mean standard errors were less than 10%.

6.1.4 MTT assay

The cytotoxicity assay was performed by measuring the viability of cells according to the method described by Denizot and Lang with slight

modification [21]. The key component (MTT) is yellowish in color and the mitochondrial dehydrogenase of viable cells cleave the tetrazolium ring, yielding purple insoluble formazan crystals, which were dissolved in a suitable solvent [22]. Then, 20 µl MTT solution (5 mg/mL in PBS) was added to each well and the plate was incubated for an additional duration of ~4 h at a temperature of 37°C followed by dissolution of the formazan crystals in DMSO. The OD at 570 nm was determined using a microplate reader to assess cell viability. The cell viability inhibitory ratio was calculated by using the formula:

$$\text{Inhibitory ratio } \% = \left(\frac{A_{control} - A_{observed}}{A_{control}} \right) \times 100 \quad (6.1)$$

6.1.5 Cell viability test

The cell viability was determined using the trypan blue exclusion assay as described in an earlier work [23]. MDA-MB231 cells were seeded in 25mm petri dish and treated with 25, 50 and 100 µg/ml of GNP and GNRs, for 24 h and at 37 °C, 5% CO_2. The cells were trypsinised and stained with trypan blue (0.4% in PBS), and counted under a light microscope by hemocytometer according to the number of viable cells that excluded trypan blue. All experiments were repeated at least three times, with the mean standard errors below 10%. The viability ratio was calculated as:

$$\% \text{ Viability ratio} = \left(\frac{\text{Observed number of viable cells}}{\text{Total number of viable cells}} \right) \times 100 \quad (6.2)$$

6.1.6 Apoptosis study by AO/EtBr

The cells were seeded on a six well plate treated with 25, 50 and 100µg/ml of GNP and GNRs, for 24 h. After the treatment, the cells were washed twice with 1X PBS and stained with 100 µl of Ethidium Bromide (10 µg/mL, HiMedia) and Acridine Orange (10 µg/mL, HiMedia) solution (1:1) and mixed gently [24]. Each sample was mixed just prior to microscopic examination and quantified immediately. The slides were placed on the platform and stained cells were examined under a fluorescence microscope (LeicaDM300, USA) with bright field and fluorescent imaging capability.

6.2 Discussion on biophysical assessment

The assessment of cytotoxicity aspect is essential when nanomaterials are considered for biological applications. Normally, free Gd^{3+} ions are toxic in nature, so ligands are chelated to reduce their toxic effect [25]. To check whether or not our RE oxide nanosystems are biocompatible, we evaluated the cytotoxicity test in peripheral blood mononuclear cell (PBMC), HepG2 and MDA-MB-231 cancer cells through MTT assays. The results of hemolysis and cell viability of cancer cells are discussed independently as follows.

6.2.1 Membrane stability test on peripheral blood mononuclear cell (PBMC) due to nano-Gd_2O_3 loading

Figure 6.1 illustrates the effect of Gd_2O_3 nanosystems on the cell viability and as a function of GNP and GNR concentrations. As for PBMC cell line response, shown in Figure 6.1 (a), the GNP and GNR were apparently non- toxic to the cells even when loaded at a very high concentration (100 μg/ml). The cell viability is retained after loading with GNP and GNRs. This indicates that the synthesized samples are extremely biocompatible below a permissible limit. The non-toxic nature is believed to be due to the Gd^{3+}ions which are strongly confined in the rigid matrices of Gd_2O_3 which the system would not release easily [26]. The biocompatibility of the nanoparticle and nanorod samples are also evaluated through the membrane stability assay. Figure 6.1 (b) and (c) depict a series of digital photographs that illustrate hemolysis results. The visual assessment of the membrane stability experiments does not show any noticeable red color in all the samples with concentration of GNP and GNR varying between 25-100 μg/ml. Apparently, the GNP and GNR samples did not exhibit any lysis of the red blood cell (RBC) membrane. However, the positive control Triton-X® treated sample exhibited a higher percentage of hemoglobin release than those treated with the Gd_2O_3 nanosystems. In other words, the GNP and GNR systems are capable of stabilizing the membrane of the RBC against rupture. Consequently, the RBC does not burst abruptly and would not allow hemoglobin to leak out of the membrane. We may also conclude that, GNP and GNR systems protect destabilization activity as caused

by the 0.1% Triton -X® on the RBC membrane. Thus both the Gd_2O_3 nanosystems exhibited outstanding compatibility with the RBC under study. The % of hemolysis in presence of GNP and GNRs, are shown independently in terms of histograms in the lower panel of the same figure. A schematic representation of hemolysis activity can be found in Figure 6.2.

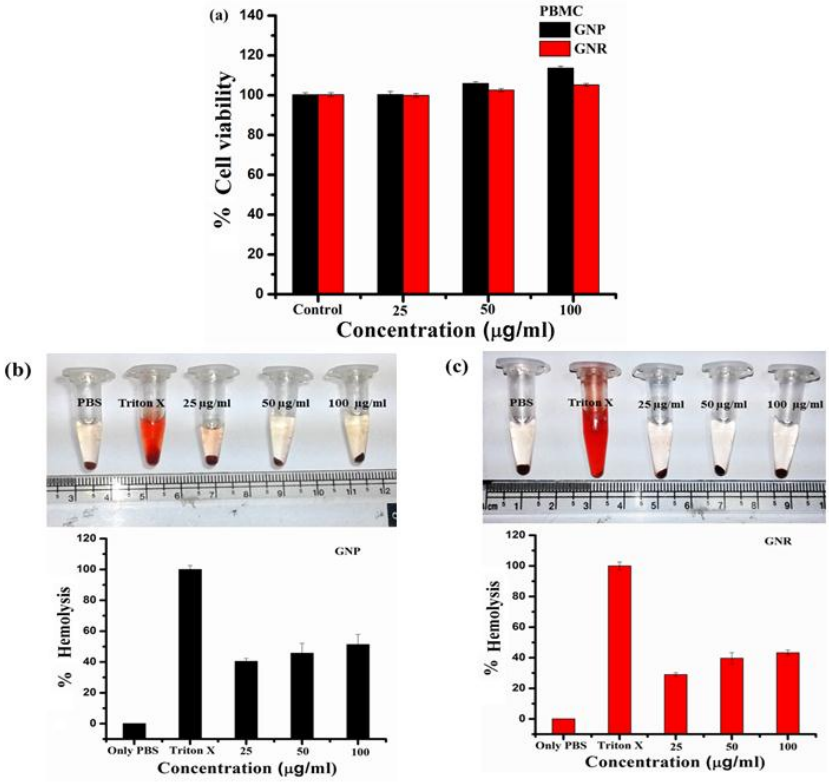

Figure 6.1:(a) Effect of GNP and GNR treatment on the cell viability of PBMC. The digital photograph and membrane stability activity of nanoparticles and nanorods are highlighted in (b) and (c); respectively.

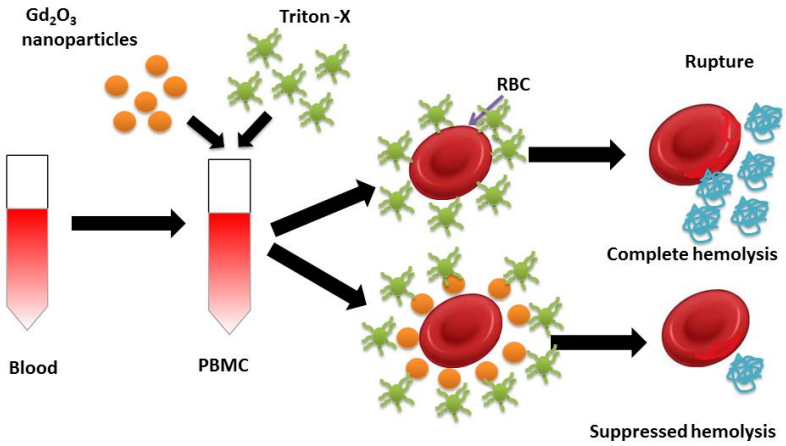

Figure 6.2: Schematic representation of hemolysis activity

6.2.2 A comparative view on cancer cell viability due to Gd_2O_3 nanoparticle and nanorod loading

To evaluate safety and nano-toxicological aspect of the prepared samples, the cytotoxicity response was examined by MTT assay using liver cancer (HepG2) and human breast cancer (MDA-MB-231) cell lines treated with various concentrations of GNP and GNRs. Figure 6.3(a) shows the representative bar-diagram that illustrates HepG2 cell line interaction with GNP (black bar) and GNR (red bar) systems. In a way, the GNRs are seen to be more efficient than GNPs since at the highest concentration (100 µg/mL), the cell viability after GNP loading is nearly 93% while after GNR loading it stands at 86%. Similarly, in case of MDA-MB-231 cell line, the cell viability delivered by GNP is ~65% in contrast to the GNR system (~57%) which gives a notably lowered value (Figure 6.3(b)). The low cell viability values of RE systems in different cell lines can be found in literature [27]. Thus the MTT based assay results suggest that, the nanoscale Gd_2O_3 systems were able to reduce the cell viability of HepG2and MDA-MB-231 cells in a concentration dependent manner, with more pronounced effect on the latter cell type.

The microscopic images of MDA-MB-231 cells incubated without and with GNP and GNR samples for 24 h are shown in Figure 6.4 (a,b). The inverted microscopic images presented in sequence indicate differences between the

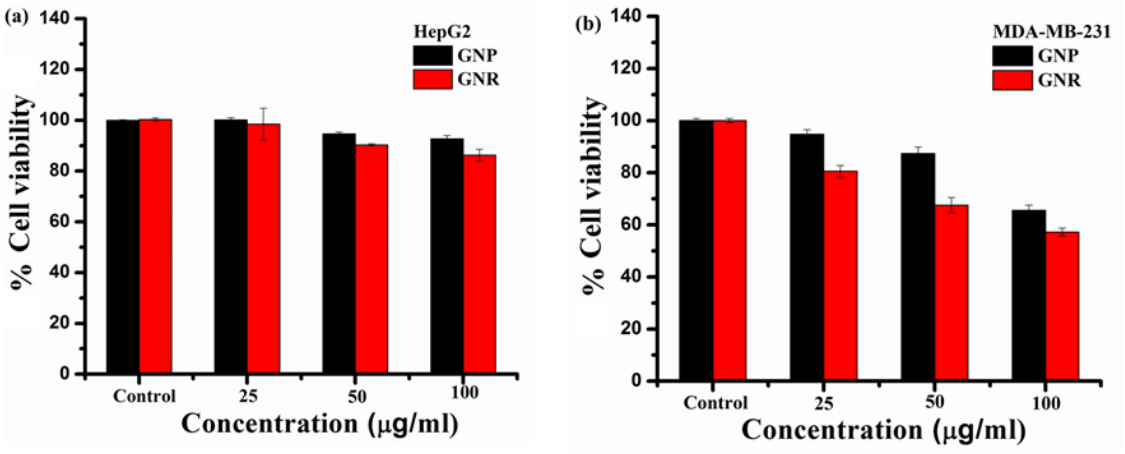

Figure 6.3: Histograms on (a) HepG2 and (b) MDA-MB-231 cell viability as measured by MTT assay with GNP and GNR loading.

controlled group and test group in cellular morphology. From the micrographs, it is quite apparent that the growth and proliferation of cancer cells is drastically suppressed upon treatment with GNP and GNR. These results also substantiate the cell viability tests by trypan blue exclusion method discussed above, thereby confirming inhibition of the growth of the breast cancer cells. The total (healthy+dead cells) and only dead cells basically correspond to blue and pink- bars in the representative histograms presented below the micrographs, and are shown for GNP (Figure 6.4(a)) and GNR (Figure 6.4(b)) in left and right columns independently.

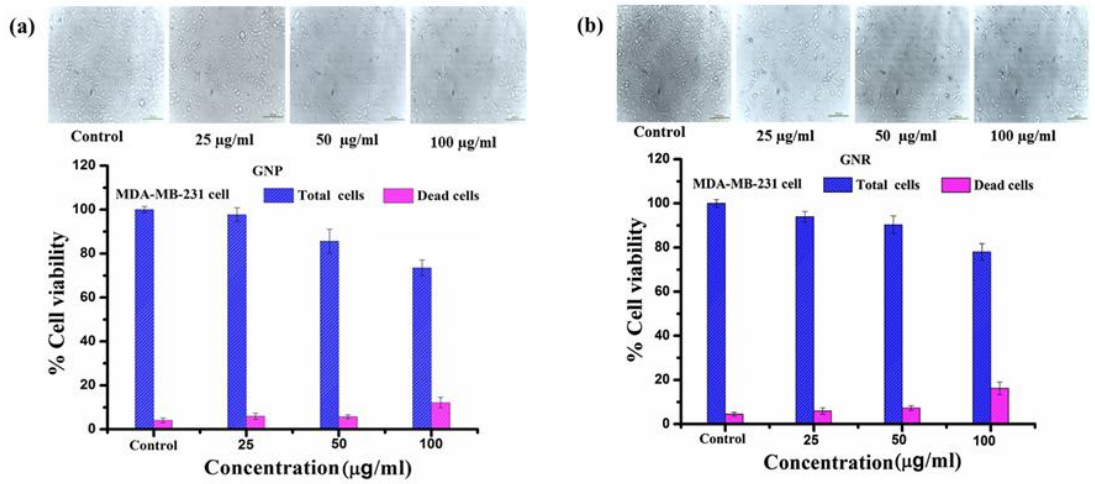

Figure 6.4: Optical microscopic images (scale bar: 100 µm) of MDA-MB-231 cells incubated without and with (a) GNP and (b) GNR treatment for 24h. Note the concentration dependent inhibition of cell growth.

A highly regulated, programmed death of cells is an important biological phenomenon called '*apoptosis*' [24]. It is a requirement for maintaining sound health of normal cells/tissue. The defective apoptotic conditions have been implicated in a wide variety of diseases, including deadly cancer. To perceive any apoptotic morphological changes induced by GNP and GNRs in MDA-MB-231 cell line, a double staining technique with ethidium bromide (EB) and acridine orange (AO) has been used. It is worth mentioning here that, the fluorescent dye AO stains both dead and live cells while EB can stain only dead cells that have lost membrane integrity. The stained cells are categorized to viable (green), early apoptotic (yellow), late apoptotic (orange) and nonviable cell (red) with bracketed colour representing fluorescence observed. Figure 6.5

signifies a comparative view on morphological changes as regards MDA-MB-231 cells with Control and GNP and GNR loading at different concentrations (25 to 100 µg/ml). The control cells were preserved without any treatment and are marked green. In contrast to control, GNP and GNR- cured cells displayed a concentration dependent decrease in viability. At high concentrations, e.g., 50 and 100 µg/ml, the GNP and GNR treatment gave ~36 and 20% and 33 and 20% early and late apoptotic cells; respectively. While 'apoptosis' represents a condition of programmed cellular death, 'necrosis' signifies abnormal death due to cellular injury or over stress. A noteworthy increase in the necrotic cells has been detected when concentration was increased from 25 to 100 µg/ml for GNP and GNR systems; respectively. An overloading of Gd_2O_3 nanosystems may have resulted in localized crowding that hampered viability and consequently, turned normal cells into necrotic ones.

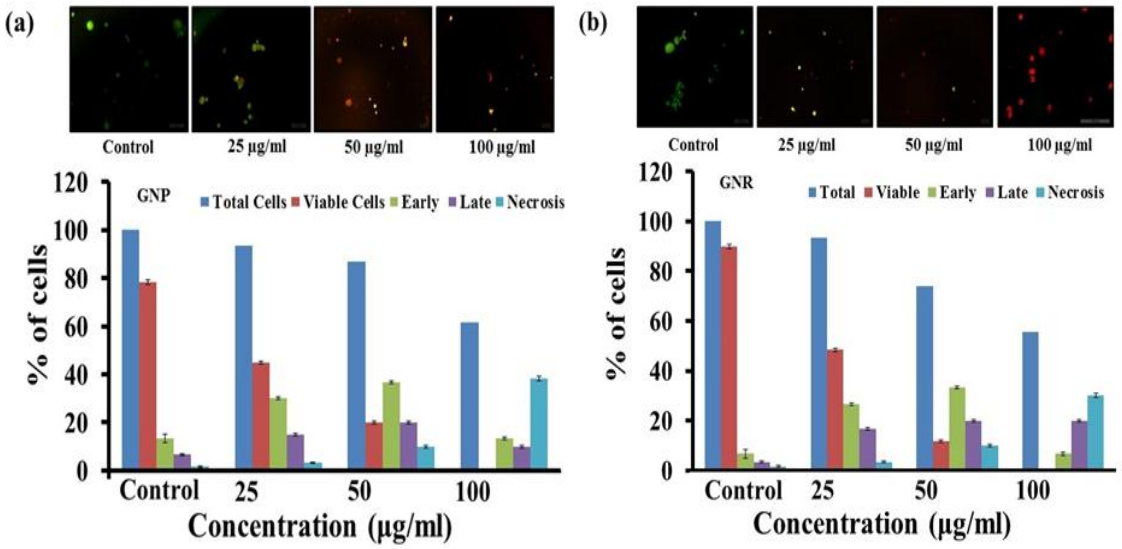

Figure 6.5 Apoptotic analysis of MDA-MB-231 cells after GNP and GNR treatment. Fluorescent images (scale bar: 100 µm) of AO/EB staining of (a) GNP and (b) GNR with different concentration of MDA-MB-231 cell lines. The colours in fluorescent images represent specific cells mentioned in the figure.

6.3 Concluding remarks

Both GNP and GNR systems (up to a concentration as high as 100 µg/mL) have not grabbed toxic effect on the PBMC cells, thereby protruding remarkable biocompatibility. An apparently observable inhibition of hemolysis along with

pronounced membrane stability authenticates safe use of nanoscale rare earth oxides; Gd_2O_3 in the present case. The synthesized nanosystems (both particles and rods) are also capable of inhibiting growth of the cancer cells (HepG2 and MDA-MB-231). While reducing the cell viability drastically, an overloading of nanosystems may result in necrosis. The anticancer efficiency of the nanoscale system might be applied in the field of cancer biology, and more specifically, in targeted therapeutics.

References

[1] Bridot, J.L., Faure, A.C., Laurent, S., Riviére, C., Billotey, C., Hiba, B., Janier, M., Josserand, V., Coll, J.L., Elst, L. V., Muller, R., Roux, S., Perriat, P., and Tillement, O. Hybrid Gadolinium Oxide Nanoparticles: Multimodal Contrast Agents for in Vivo Imaging. *Journal of the American Chemical Society,* 129: 5076-5084, 2007.

[2]Petoral, J. R.M., Söderlind, F., Klasson, A., Suska, A., Fortin, M.A., Abrikossova, N., Selegård, L., Käll, P.O., Engström, M., and Uvdal, K. Synthesis and characterization of Tb^{3+}-doped Gd_2O_3 nanocrystals: A bifunctional material with combined fluorescent labeling and MRI contrast agent properties. *Journal of Physical Chemistry C,* 113: 6913 -6920, 2009.

[3] Riegler, J., and Nann, T. Application of luminescent nanocrystals as labels for biological molecules. *Analytical and Bioanalytical Chemistry*, 379: 913-919, 2004.

[4] Torsello, G. Lomascolo, M., Licciulli, A., Diso, D., Tundo S., and Mazzer, M. The origin of highly efficient selective emission in rare-earth oxides for thermophotovoltaic applications. *Nature Materials* 3: 632-637, 2004.

[5] Bai, L., Liu, J., Li, X., Jiang, S., Xiao, W., Li, Y., Tang, L., Zhang, Y., and Zhang, D.Pressure-induced phase transformations in cubic Gd_2O_3. *Journal of Applied Physics,* 106: 073507(1-4), 2009.

[6]Guo, H., Dong, N., Yin, M., Zhang, W., Lou, L., and Xia. S. Visible Upconversion in Rare Earth Ion-Doped Gd_2O_3Nanocrystals .*Journal of Physical Chemistry B*, 108: 19205-19209, 2004.

[7]Wagoner ,M. Van. and Worah, D. Gadodiamide Injection: First Human Experience with the Nonionic Magnetic Resonance Imaging Enhancement Agent. *Investigative Radiology*, 28: S44–S48, 1993.

[8] Park, J. Y., Baek, M. J., Choi, E. S, Woo, S., Kim, J. H., Kim,T. J., Jung, J. C., Chae, K. S., Chang, Y., and Lee, G. H. Paramagnetic ultrasmall gadolinium oxide nanoparticles as advanced T1 MRI contrast agent: Account for large longitudinal relaxivity, optimal particle diameter, and in vivo T1 MR images. *ACS Nano* 3: 3663-3669, 2009.

[9] Caravan, P. Ellison, J. J., McMurry, T.J., and Lauffer, R. B. Gadolinium(III) Chelates as MRI Contrast Agents: Structure, Dynamics, and Applications. *Chemical Reviews,* 99: 2293–2352, 1999.

[10] Soto, K., Garza, K.M., and Murr L.E. Cytotoxic effects of aggregated nanomaterials. *Acta Biomaterialia* 3: 351–358, 2007.

[11] Moss, O. R. Insights into the health effects of nanoparticles: why numbers matter. *International Journal of Nanotechnology,* 5: 3–14, 2008.

[12] Panessa-Warren, B. J., Warren, J, B., Maye, M. M., Lelie, D. V. D., Gang, O., Wong, S., Ghebrehiwet, B., Tortora, G., and Misewich, J. Human epithelial cell processing of carbon and gold nanoparticles. *International Journal of Nanotechnology*, 5: 55–91, 2008.

[13] Stolle, L. B., Hussain, S., Schlager, J. J., and Hofmann, M.C. In vitro cytotoxicity of nanoparticles in mammalian germline stem cells. *Toxicological Sciences,* 88:412–419, 2005.

[14] Heinrich, M. C. et al. Kuhlmann, M. K., Kohlbacher, S., Scheer, M., Grgic, A., Heckmann, M. B., and Uder, M. Cytotoxicity of Iodinated and Gadolinium-based Contrast Agents in Renal Tubular Cells at Angiographic Concentrations: In Vitro Study. *Radiology,* 242: 425–434, 2007.

[15] Das,G. K., Zhang, Y., D'Silva, L., Padmanabhan, P., Heng, B. C., Loo, J. S. C., Selvan, S. T., Bhakoo,K. K., and Tan, T. T. Y. Single-phase Dy_2O_3:Tb^{3+} nanocrystals as dual-modal contrast agent for high field magnetic resonance and optical Imaging. *Chemistry of Materials,* 23: 2439–2446, 2011.

[16] Medintz, I.L., Uyeda, H. T., Goldman, E. R., and Mattoussi, H. Quantum

dot bioconjugates for imaging, labelling and sensing. *Nature Materials*, 4: 435-446, 2005.

[17] Michalet, X., Pinaud. F. F., Bentolila, L. A., Tsay, J. M., Doose. S., Li, J. J., Sundaresan, G., Wu, A. M., Gambhir, S. S., and Weiss, S. Quantum dots for live cells, *in vivo* imaging, and diagnostics. *Science* 307: 538-544, 2005.

[18] Menon, J.U., Jadeja, P., Tambe, P., Vu, K., Yuan, B., and Nguyen, K. T. Nanomaterials for photo-based diagnostic and therapeutic applications. *Theranostics* 3 :152-166, 2013.

[19] Gómez-Lechón, M. J., Iborra, F. J., Azorin, I., Guerri, C., and Renau-Piqueras, J. Cryopreservation of rat astrocytes from primary cultures. *Journal of tissue culture methods*, 14: 73–77, 1992.

[20]Vargas,F. de S., Almeida ,P. D. O. de., Aranha , E. S. P., Boleti, A. P. A., Newton, P., Vasconcellos, M. C. ., Junior, V. F. V and Lima, E. S. Biological Activities and Cytotoxicity of Diterpenes from Copaifera spp. Oleoresins. *Molecules* 20: 6194-6210, 2015.

[21]Denizot, F., and Lang, R. Rapid colorimetric assay for cell growth and survival Modifications to the tetrazolium dye procedure giving improved sensitivity and reliability. *Journal of Immunological Methods,* 89: 271–277, 1986.

[22] Lee, J. W., Serna, F., Nickels, J., Schmidt, C.E. Carboxylic acid-functionalized conductive polypyrrole as a bioactive platform for cell adhesion. *Biomacromolecules,* 7:1692-1695,2006.

[23] Sun, Y. Zou , M., Hu, C., Qin, Y., Song, X., Lu, N., and Guo, Q. Wogonoside induces autophagy in MDA-MB-231 cells by regulating MAPK-mTOR pathway, *Food and Chemical Toxicology,* 51: 53–60, 2013.

[24] Ebrahim, K., Shirazi, F.H., Vatanpour, H., Zare, A., Kobarfard, F., and Rabiei, H. Anticancer Activity of Cobra Venom Polypeptide, Cytotoxin-II, against Human Breast Adenocarcinoma Cell Line (MCF-7) via the Induction of Apoptosis. *Journal of Breast Cancer,* 17:314-322, 2014.

[25] Li, W.-h., Fraser, S. E., and Meadet, T. J. A Calcium-Sensitive Magnetic Resonance Imaging Contrast Agent. *Journal of the American Chemical Society,* 121: 1413-1414**,** 1999.

[26] Zhou, L., Gu, Z., Liu, X., Yin, W., Tian, G., Yan, L., Jin, S., Ren, W., Xing, G., Li, W., Chang, X., Hu, Z and Zhao, Y. Size-tunable synthesis of lanthanide-doped Gd_2O_3 nanoparticles and their applications for optical and magnetic resonance imaging. *Journal of Materials Chemistry,* 22: 966–974, 2012.

[27] Das, G. K., Chan, P.P., Teo, A., Loo, J.S., Anderson, J.M., and Tan, T.T. In vitro cytotoxicity evaluation of biomedical nanoparticles and their extracts. *Journal of Biomedical Materials Research Part A* , 93: 337-346, 2009.